An Approach to Evaluating the Impact of Small-core Turbofan Technologies on Engine and Aircraft Performance

Michael A. Bennett* and Jeffryes W. Chapman †
NASA Glenn Research Center, Cleveland, OH, 44135, USA

Douglas P. Wells‡
NASA Langley Research Center, Hampton, VA, 23681

NASA's Hybrid Thermally Efficient Core (HyTEC) project aims to accelerate the development of small-core turbofan engine technologies to enable a fuel burn reduction of 5 to 10 percent for next-generation aircraft, compared to 2020s best-in-class technology. This paper presents a demonstration of methods for evaluating the potential performance impact of small-core engine technologies developed under Phase 1 of the HyTEC project. The approach involves model-based systems analysis, where small-core innovations are integrated into baseline turbofan and aircraft systems models, creating a notional vision system. Performance of the vision system is examined at both the engine and vehicle level. The examined performance metrics include: engine bypass ratio, overall pressure ratio, high pressure compressor exit corrected mass flow, and aircraft fuel burn. The CFM LEAP-1B28 and Boeing 737 MAX 8 are chosen as the baseline state-of-the-art systems. Preliminary results map a design space for the small-core vision system and quantify the distinct effects of technologies on the key metrics.

I. Nomenclature

$\dot{m}_c$	Corrected mass flow rate
T	Total temperature
TSFC	Thrust specific fuel consumption
V	Velocity
α	Bypass ratio
η	Efficiency, Adiabatic efficiency
λ	Thrust lapse

Subscripts

19	Engine cycle station 19, bypass nozzle exit
3	Engine cycle station 3, high pressure compressor exit
4	Engine cycle station 4, high pressure turbine inlet
41	Engine cycle station 41, high pressure turbine blade row 1 inlet
9	Engine cycle station 9, core nozzle exit
$poly$	Polytropic efficiency

II. Introduction

The Sustainable Flight National Partnership (SFNP) is a collaborative effort between NASA Aeronautics, industry, academia, and other agencies to achieve the U.S. aviation climate goal of net-zero greenhouse gas emissions from the aviation sector by 2050 [1]. This partnership aims to promote the development and deployment of sustainable aviation technologies that can help reduce the environmental impact of aviation. In support of this effort, NASA is working

*Aerospace Engineer, Propulsion Systems Analysis Branch, 21000 Brookpark Rd., AIAA Member
†Aerospace Engineer, Propulsion Systems Analysis Branch, 21000 Brookpark Rd., AIAA Member
‡Aerospace Engineer, Aeronautics Systems Analysis Branch, Mail Stop 442, AIAA Senior Member.

with industry partners under the Hybrid Thermally Efficient Core (HyTEC) project to accelerate the development and demonstration of advanced, high-power density, small-core gas turbine engine technologies. As a key steppingstone towards achieving the goals of the SFNP, the HyTEC project aims to enable a 5 to 10 percent reduction in fuel burn for the next single-aisle commercial aircraft, anticipated to enter into service (EIS) in the 2030s, versus a comparable 2020s best-in-class vehicle [2].

To achieve the objective fuel burn reduction, the focus of the HyTEC project is to develop technologies that enable a size reduction of an engine's high-pressure compressor (HPC), burner, and high pressure turbine (HPT) components - collectively referred to as the core of the engine. Reducing the size of the core while maintaining a sufficient power output permits the design of propulsion systems with a higher bypass ratio (BPR) and improved overall efficiency. Under Phase 1 of the HyTEC project, NASA has invested in developing a suite of compact core technologies at the component or subsystem level to a technology readiness level (TRL) of 4 to 5 to tackle some of the technical challenges specifically related to reducing the engine core size including [3]:

- High Pressure Compressor – Casing treatments and advanced designs to enable operability with optimized efficiency and performance
- Enhanced Combustor Materials – Ceramic matrix composite (CMC) liners for combustors to increase performance and durability
- High Temperature Turbine Materials – CMCs and environmental barrier coatings (EBCs) for turbine blades and vanes to increase temperature limitations and efficiency
- High-Pressure Turbine Aerodynamics – Advanced turbine blade aerodynamic features and cooling designs to enable more efficient operation

Advancements made during the HyTEC technology development activities are measured, in part, using the Key Performance Parameters (KPPs) listed in Table 1 [2]. This paper presents a demonstration of the methods employed to investigate the influence of HyTEC Phase 1 small-core technologies on a selection of these KPPs for a baseline 2020s state-of-the-art (SOA) turbofan and single-aisle aircraft. Furthermore, it offers an initial exploration of the potential technology performance benefit trends. Of the KPPs listed in Table 1, the ones examined in this study include: aircraft overall fuel burn, engine BPR, engine overall pressure ratio (OPR), and HPC exit corrected mass flow. The KPP metrics are evaluated by comparing two systems: a baseline, or reference, system and an advanced (EIS 2035) vision system with small-core technologies. The CFM LEAP-1B28 turbofan (LEAP) and Boeing 737 (B737) MAX 8 are used as the reference baseline SOA systems. All gas turbine engine cycle simulations are carried out using the Numerical Propulsion System Simulation code [4]. Engine weight estimates are evaluated using the Weight Analysis of Turbine Engines (WATE++) code [5], and aircraft performance is examined using the Flight Optimization System (FLOPS) program [6]. All analyses for this paper are carried out using only publicly sourced information and data. This is done in the interim, pending an official HyTEC technology benefit assessment that will be completed using experimental data from the technology development activities, and released as an unlimited rights agreement with contracted technology developers.

Table 1 HyTEC Project Key Performance Parameters [2]

Key Performance Parameter #	Key Performance Parameter	Full Success Single Aisle ~2035 EIS	Minimum Success Single Aisle ~2035 EIS
KPP-1	Fuel burn reduction attributed to the high-power density core of the original equipment manufacturer's (OEM) vision turbofan engine	10%	5%
KPP-2	Engine Bypass Ratio	> 15	> 12
KPP-3	Engine Overall Pressure Ratio (Defined at top of climb)	> 50	> 45
KPP-4	Durability, measured in operating hours between major refurbishment	Exceed SOA by 5%	Meet SOA of baseline
KPP-5	Degree of hybridization measured by level of power extraction from the turbofan engine at altitude	20%	10%
KPP-6	HPC Exit Corrected Flow	< 3 lbm/s	< 3.5 lbm/s

III. Assumptions

A. Baseline engine and aircraft

The notional small-core engine developed in this study is a two-spool turbofan engine with features that make it an evolution of the LEAP turbofan. The engine is sized to meet the thrust requirements of a B737 MAX 8 class vehicle, and is hereafter referred to as the 'vision' engine. As the study's goal is to forecast the potential progress that small-core technologies will make towards achieving the HyTEC KPPs, in-house numerical models of the LEAP and B737 MAX 8 are used to benchmark KPPs. These models were calibrated simultaneously to match performance data found in public documents such as the engine Type Certification Data Sheet [7], emissions data sheet [8], and airport planning documentation [9]. These current technology models are hereafter referred to as the 'baseline' (or 'reference') engine and vehicle. More detailed information about the calibration of these specific models can be found in Ref. [10]. Figure 1 shows a block diagram of the in-house baseline NPSS model. The green boxes represent where fluid enters or leaves the systems; the blue boxes represent components which fluid passes through; and the orange boxes represent shaft connections. Table 2 lists the baseline KPP values and other important performance parameters for the reference engine model at pertinent operating conditions.

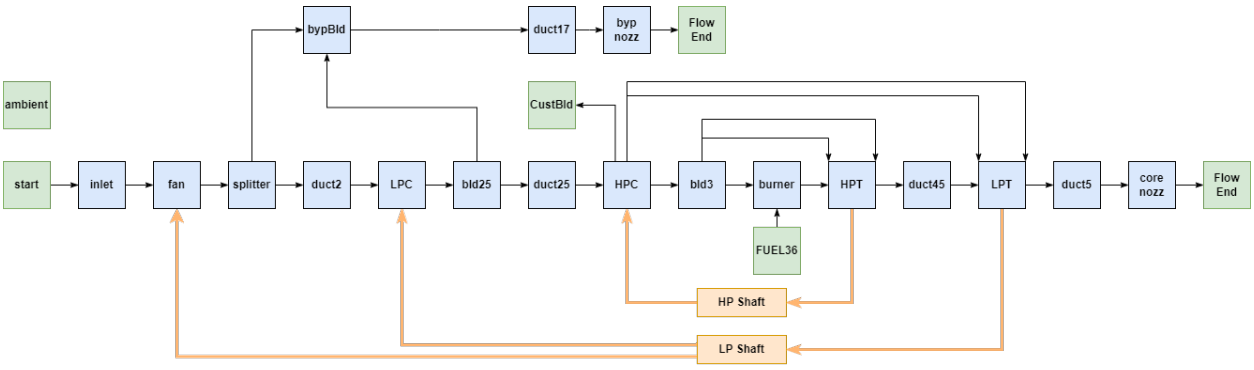

Fig. 1 Block Diagram of the reference NPSS model

The reference aircraft in this study is a model of the B737 MAX 8 airplane. The weight and mission performance were modeled in FLOPS and were calibrated using a collection of public data to accurately simulate the performance of the B737 MAX 8. Figure 2 shows an OpenVSP [11] render of the B737 MAX 8 model. Table 3 lists the parameter values for the calibrated B737 MAX 8 like aircraft model.

Table 2 Reference Engine Model Data

Parameter	Model Results	Notes
Takeoff thrust rating (lbf)	29,317	Uninstalled thrust
Bypass ratio	8.6	At sea level static, uninstalled
Overall pressure ratio	44.6	At Top of Climb
HPC exit corrected mass flow (lbm\s)	4.23	At Cruise
TSFC	0.56	At Cruise
Total engine pod weight (lbf)	8050	
Fan diameter (in)	69.4	

Table 3 Reference Aircraft Model Data

Parameter	Model Results
Max Design TOGW (lb)	182,200
Max Payload (lb)	46,040
Number of Passengers	169
Design Range (nmi)	3,500
Design Range Block Fuel (lb)	38,857
Economic Range (nmi)	1,000
Economic Range Block Fuel (lb)	9,664
Wing Area (ft^2)	1,370
Wing Span (ft)	118
Aspect Ratio	11.2
Wing Loading (lb/ft^2)	133
Cruise Mach	0.78
Max Operating Mach	0.82

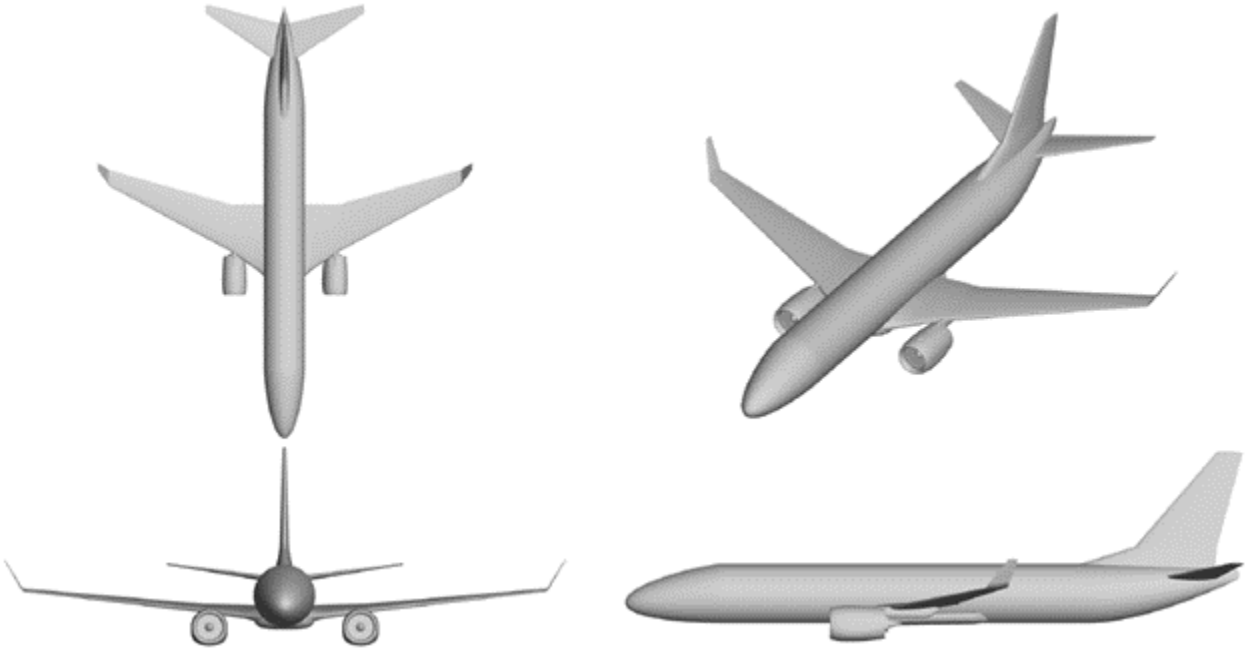

Fig. 2 OpenVSP [11] render of the reference aircraft used to define the geometric inputs to FLOPS.

B. Vision engine cycle design

The design space of a vision engine is explored using a multiple design point (MDP) approach [12]. Many of the design rules and assumptions used during the calibration of the reference engine model are used for the vision cycle design to facilitate the design of an engine that is an evolution of current technology, and to ensure that the system is capable of powering a B737 class aircraft. Table 4 provides a summary of the engine operating points considered during the cycle design, and the net thrust assumed to be required at these points. The net thrust required at sea level static, uninstalled, (SLSUI) is 29,317 lbf [7][8]. For SLSUI, the atmospheric condition is set to standard-day, and there is no pressure loss through the inlet. For the sea level static installed condition (SLS) the atmospheric condition is set to hot-day, and a pressure loss is applied through the inlet. Engine airflow is adjusted to achieve the net thrust required at SLS–28,928 lbf [9]. At SLS, the turbine inlet temperature T_4 is modified to provide the net thrust required at rolling takeoff (RTO). The net thrust requirement at RTO is based the Boeing Equivalent Thrust target ($F_{\text{n,SLS}}/1.2553$) [13]. At top of climb (TOC), fuel flow is adjusted to achieve a thrust target set using a thrust lapse factor λ. The thrust requirement at CRS is targeted to be 90% of the TOC thrust. The pressure ratios of the fan and the compressors (i.e. OPR) are set at the TOC condition. The adiabatic efficiencies of the turbomachinery are set at the TOC condition, and may be adjusted to achieve polytropic efficiency values targeted at the CRS condition. The design efficiency of the HPT is adjusted as a function of the amount of turbine cooling air (TCA) required. The method used to adjust turbine efficiency is detailed later in Section IV.A. The amount of TCA required is calculated using the algorithm described in Ref. [14], and is largely a function of T_4 and the allowable HPT blade and vane material temperatures $T_{\text{metal, HPT}}$. Cooling flow requirements for the HPT are determined at RTO, and is set as a fraction of the station 25 mass flow. The gas temperature at the entrance of the HPT stage 1 blades T_{41} is influenced by both T_4 and the quantity of TCA directed to the HPT. The fuel flow rate at RTO is regulated to attain a maximum permissible T_{41}. To observe how the integration of small-core technologies influences the cycle BPR, the design BPR is set as an independent variable which is varied to achieve a prescribed ratio between the core and bypass exhaust velocities (V_9/V_{19}).

Table 4 Vision Cycle Design Points

Design Point	Altitude (ft)	Atmosphere	M_0	$F_{\mathbf{n}}$ (lbf)
Top of Climb	35,000	Standard Day	0.79	$\lambda F_{\text{n, SLS}}$
Cruise	35,000	Standard Day	0.79	$0.9F_{\text{n, TOC}}$
Rolling Takeoff	0	Hot Day	0.25	$F_{\text{n, SLS}}/1.2553$
Sea Level Static	0	Hot Day	0.0	28,928
Sea Level Static Uninstalled	0	Standard Day	0.0	29,317

C. Engine flowpath and weight estimation

Engine size and weight are critical measures to consider when assessing fuel burn at the vehicle level. To evaluate how small-core technologies may influence these measures, estimations of engine weight and flowpath dimensions are formulated for the vision engine using the NASA's Weight Analysis of Turbine Engines tool, WATE++. The essential cycle parameters required for the execution of WATE++, such as air mass flow, maximum operational temperatures, and pressures, are extracted from the NPSS thermodynamic cycle output. The cycle data used includes data from both the aerodynamic design point (TOC) and a range of off-design scenarios, including SLS and RTO, which ensure the inclusion of the most extreme thermodynamic conditions that could be encountered by the engine. The cycle data is used in conjunction with material properties and principles governing component design in order to establish a feasible engine flowpath. These design principles take into account various constraints, including geometric limitations, stress thresholds, and the loading capacities of different turbomachinery stages.

Just as the vision thermodynamic cycle is derived using the baseline LEAP-like cycle model, estimations of the vision engine's weight and flowpath are derived from modifications made to a LEAP-like WATE++ model. The construction of the baseline WATE++ model is modified to consider the use of small-core technologies such as lightweight materials and improved stage loading capabilities. By this method, the WATE++ results produced for the vision engine are influenced by both aeromechanical design changes, and differences between the baseline and vision systems' thermodynamic cycle outputs.

D. Aircraft Integration

The study's goal is to forecast the potential progress that small-core technologies will make towards achieving the HyTEC project's KPPs. Therefore, a fixed aircraft model is used to isolate the impacts from changes to the engine model. The vision engine is integrated into the reference, B737 MAX 8 like, aircraft model to generate the total vehicle performance. The vision engine cycle results along with the WATE++ results are used to install the vision engine into the reference aircraft model; the aircraft mission rules and geometry are unchanged. This enables the results comparison to reflect impacts from the vision engine model versus the reference engine model. The vision engine model results are shown as the re-engine B737 MAX 8 like FLOPS model.

IV. Technology Integration Methods and Sensitivities

A. Technology integration

Much of the detailed information concerning the technology enhancements being pursued within HyTEC is of a proprietary nature. In the interim, the technology improvements integrated for the vision cycle primarily draw from research conducted during or after NASA's Environmentally Responsible Aviation project [15], along with the envisioned technological progress for the N+3 timeframe (EIS 2030-2035) [16]. These advancements encompass enhanced aerodynamics for turbomachinery, innovative methods for turbine cooling, and the utilization of CMC materials. Excluded from consideration are technologies that exist outside the LEAP engine, or that are envisioned for future propulsion systems. These concepts include geared or unducted fans, intercooled or regenerative cycles, hybrid electric systems, and alternative aviation fuels. Furthermore, minimal technology improvements are considered for the low pressure spool turbomachinery. This is done in an effort to isolate the influence of core technology integration on engine performance. Based on these considerations, the component-specific performance of the baseline engine model is modified as follows to explore the design space of a vision cycle, and to assess the sensitivity of the HyTEC KPPs to variations made to these cycle design parameters.

Fan

The vision cycle fan is unchanged from the baseline engine model. The maximum fan pressure ratio is approximately 1.6. The fan diameter is constrained to 69.4 inches, as to not exceed the diameter of the LEAP.

Low Pressure Compressor

The vision cycle LPC is unchanged from the baseline engine model. The pressure ratio is around 1.25 and the peak polytropic efficiency is approximately 88%.

High Pressure Compressor

The integration of small-core HPC technologies may be represented by adjustments made to the baseline engine's HPC pressure ratio and efficiency. To explore cycles with an OPR as high as 50 (HyTEC KPP-3, full success), the HPC pressure ratio is adjusted to values within the range of around 22 (baseline) to 25. The design polytropic efficiency remains consistent across different core sizes and is maintained at the value employed in the baseline model—92%. Typically, when core size is reduced, a decrease in polytropic efficiency would be considered to account for increased losses stemming from the reduction in flow area at the rear of the compressor. These losses could be due to factors like tip clearance scaling, effects from low Reynolds numbers, or limitations in airfoil geometry due to manufacturing constraints. However, by keeping the polytropic efficiency constant, it is assumed that advancements in compressor technologies, such as improved aerodynamics or innovative casing treatments, will counterbalance these losses. Although this might seem like an ambitious approach, it is not overly aggressive. Predictions of polytropic efficiency trends relative to core size suggest that reducing the core size from 4.23 (baseline) to 3.0 would result in a polytropic efficiency loss of less than 1.5%[17].

Combustor

The burner of the vision cycle uses a CMC liner for improved durability and reduced weight. The analysis presented here does not consider the effects of combustor technologies on cycle performance. Any fuel burn benefit that is quantified for the burner is attributed to its reduced weight. The stagnation pressure drop across the burner is about 4%.

High Pressure Turbine

The HPT consists of a two-stage turbine with a baseline adiabatic efficiency of approximately 91%. The HPT of the advanced cycle is envisioned to employ CMC vanes, advanced EBCs, and advanced airfoil designs with improved cooling features. The integration of these technologies may improve a turbine's operability and efficiency at elevated temperatures. To explore the design space of the advanced cycle, HPT adiabatic efficiencies up to 95% are investigated. Additionally, the maximum HPT stage 1 blade inlet temperature $T_{41,\max}$, and the maximum HPT blade material temperature $T_{\text{metal, HPT}}$ are increased by up to 300°F compared to the temperatures employed by the baseline model [18]. The advanced cycle is modeled such that variations in $T_{41,\max}$ and $T_{\text{metal, HPT}}$, relative to the baseline values, influence the amount of TCA required.

Two methods are considered when modifying the baseline HPT efficiency. The first approach employs a simple technique, wherein the base HPT efficiency is manually increased to simulate the integration of some HPT technology, such as a blade aerodynamic design improvement, which enhances turbine efficiency while maintaining the same baseline cooling level. In the second approach, the baseline HPT efficiency is modified based on the amount of TCA required. This method is used to simulate the effects of cooling on turbine efficiency. The extent to which cooling air influences turbine efficiency is contingent upon various factors and can significantly vary depending on the specific cooling method considered (e.g., surface film, trailing or leading edge cooling, etc.). Consequently, experimental data and validation are often required to accurately estimate losses in turbine efficiency due to cooling. Some estimations in literature show that, depending on the cooling feature used, the adiabatic efficiency of an uncooled turbine may be debited by about 0.25% to 1.5% per percent of cooling flow [19][20]. In the analysis presented here, there is no assumption made for the specific type of cooling flow that may be reduced as the result of a small-core technology development. Instead, a simplified assumption is made for the exchange rate between TCA and HPT efficiency, where a complete reduction in TCA would improve the baseline HPT adiabatic efficiency up to maximum value of 95% for the advanced cycle. When this technique is used, the baseline HPT efficiency is adjusted by 0.04% per 1% relative change in TCA. When this rate is expressed in terms of an absolute percent reduction of TCA, the rate falls within the range of those found in literature.

Figure 3 portrays the relationship between adjustments to $T_{41,\max}$ and $T_{\text{metal, HPT}}$ and their influence on the TCA requirement of the reference engine model. Also shown is the assumed trend in HPT efficiency, which is a result of changes in the TCA demand. The figure shows that improvements in $T_{\text{metal, HPT}}$ reduce the amount of cooling required, while the required cooling increases at heightened $T_{41,\max}$. A material temperature improvement of 300°F results in a TCA reduction of about 60%, corresponding to a maximum attainable HPT adiabatic efficiency of about 93.5%. A gas temperature improvement (increase) of 300°F results in a TCA increase of about 70%. Note that the slope of the $\Delta TCA = 0\%$ line is not 1. This is because the cooling air becomes more effective at higher temperatures due to the decreasing relative temperature as T_{41} becomes hotter. Thus, for roughly no change in TCA, a gas temperature increase of 300°F could be accommodated with a 200°F increase in material temperature.

Low Pressure Turbine

The LPT is a cooled five-stage turbine with a polytropic efficiency of approximately 90%. The amount of cooling air required and the design efficiency are not modified from the values used in the base model. Stage loading is improved to eliminate the need for an increased stage count at higher BPR. It is assumed that the technological enhancements required to increase the LPT stage loading have been introduced, and that these changes have a negligible impact on the turbine's efficiency

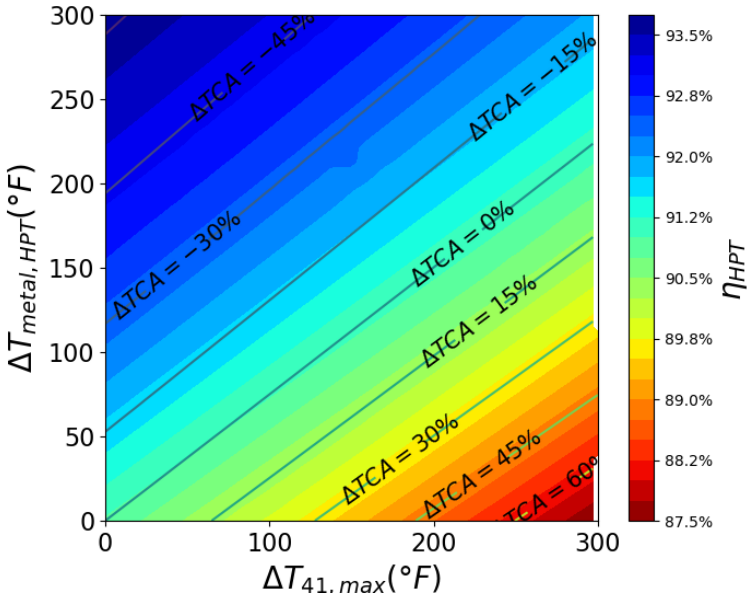

Fig. 3 Trend of HPT cooling air required and assumed trend of HPT adiabatic efficiency.

B. KPP sensitivity studies

The previous section outlined which cycle design parameters would be altered to represent the integration of a small-core technology into the baseline propulsion system, and the extent to which these parameters would be modified to map the design space of the vision engine. In this section, the performance trends which result from implementing these cycle design changes are presented. All analyses are executed using the cycle design methodology detailed in Section III.B.

High Pressure Compressor Technologies

Figure 4 displays the KPP trends when considering adjustments made to OPR at three constant values of HPC polytropic efficiency. Changes to OPR are made by adjusting the HPC pressure ratio exclusively. The cycle OPR is increased up to 50 from a baseline value of 44.6. The three polytropic efficiency values utilized consider a potential decrease or enhancement of 1% compared to the baseline value of 92%. The results show that approximately a 1% change in TSFC (i.e. fuel burn) can result from a 1% change in polytropic efficiency. This result highlights the importance of mitigating efficiency losses in a small-core compressor. A reduction in TSFC and core size is shown to be the result for any increase of OPR, indicative of improved thermal and overall efficiency. TSFC reduces at a rate of about 0.05% per 1% rise in OPR. Core size decreases at a rate of approximately 0.025 lbm/s per 1% increase in OPR. Noticeably, Fig. 4 shows that BPR slightly decreases with heightened OPR. As OPR is improved, the specific power of the core decreases because the assumption of a constant T_{41}. As such, a slight increase in mass flow through the core is required to achieve the design jet velocity ratio and net thrust. Overall, when only considering the integration of compressor technologies, it is evident that the gains in overall performance fall below the standards set by the HyTEC KPPs.

High Pressure Turbine Technologies

The KPP trends which result from integrating HPT technologies that enhance turbine efficiency while maintaining the same baseline cooling level are presented by Fig. 5. For this exercise, the HPT efficiency is increased manually up to a value of 95%, and $T_{41,\max}$ is increased by up to 300°F. Results are provided considering two different OPRs: the baseline OPR of 44.6, and the HyTEC full success OPR of 50. In both the baseline and the high OPR case, it is shown that TSFC is reduced at elevated HPT efficiency and improved $T_{41,\max}$, showcasing the complimentary influence of these two parameters on thermal and overall efficiency. Figure 5a shows that when HPT efficiency is increased at the

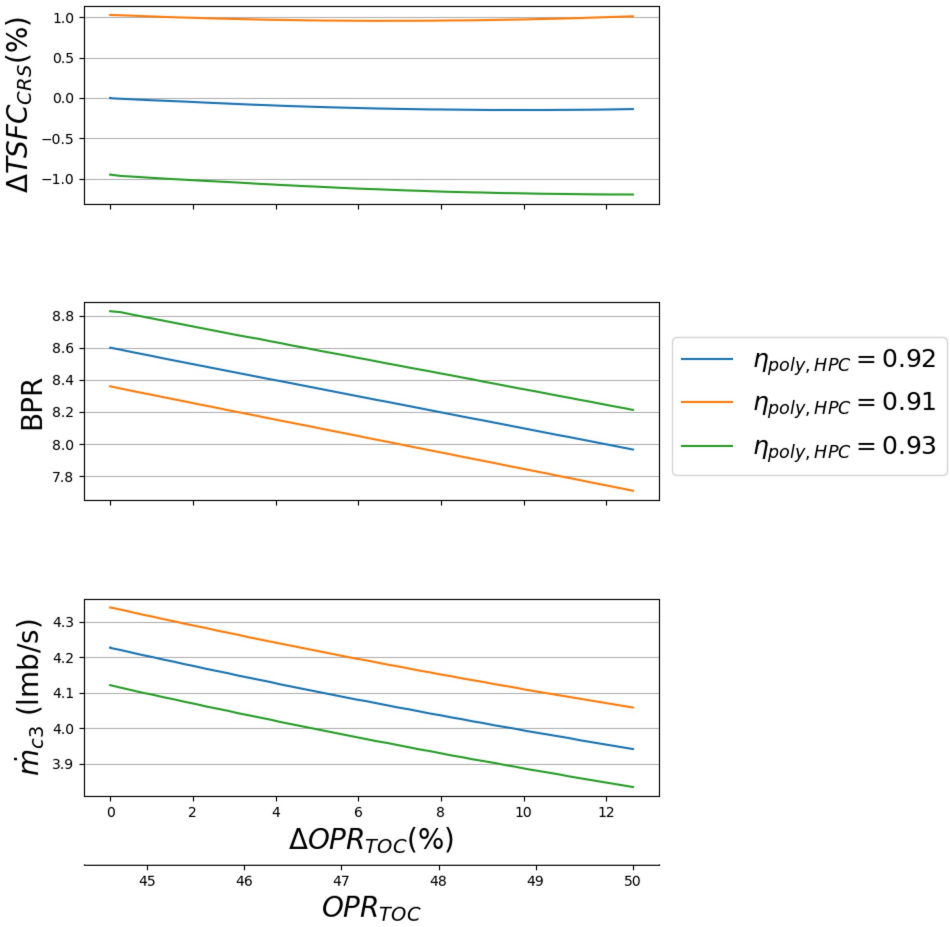

Fig. 4 KPP sensitivity to increased OPR at different values of HPC polytropic efficiency

base $T_{41,\max}$, the core size remains greater than 4.0 lbm/s, the BPR (denoted by α) is less than 9.0, and TSFC is reduced by up to 2.8%. When both HPT efficiency and $T_{41,\max}$ are increased to the full potential, core size is reduced to around 3.3 lbm/s, BPR increases to approximately 11.5, and TSFC is reduced by 4.1%. By Fig. 5b it is unsurprisingly revealed that the benefits of increased cycle temperature are more profound at a heightened OPR. At an OPR of 50, and when both HPT efficiency and $T_{41,\max}$ are increased to the full potential, core size is reduced below 3.1 lbm/s, BPR increases to around 11.0, and TSFC is reduced by 5.3%. While these outcomes for core size reduction and fuel burn reduction would satisfy HyTEC's minimum success criteria, it's important to note that significantly raising the maximum cycle temperature would likely necessitate a more substantial degree of turbine cooling. Consequently, this would likely hinder the ability to improve HPT efficiency to the extent that is explored here.

Considering the KPP of BPR, Fig. 5b reveals that even for the most ambitious of scenarios, where core size is reduced to nearly 3.0, the BPR of any vision cycle is not likely to exceed the minimum success criteria for HyTEC–BPR>12. It is possible that modifying the jet velocity ratio used for the cycle design could increase the BPR achievable for the advanced cycle, but it is probable that other engine technologies which increase propulsive efficiency will need to be considered to increase the BPR beyond 12 (e.g. reduced fan pressure ratio, geared turbofan).

The KPP trends which result from integrating HPT technologies that enhance $T_{41,\max}$, and the allowable $T_{\text{metal, HPT}}$ are shown by Fig. 6. Four different cases are presented. In Fig. 6a and Fig. 6b the influence of temperature variations on TCA requirements is considered, but the assumed effects of TCA on HPT efficiency, detailed in Section IV.A, are not accounted for. The baseline HPT adiabatic efficiency, 91%, is employed. The assumed effects of TCA on HPT

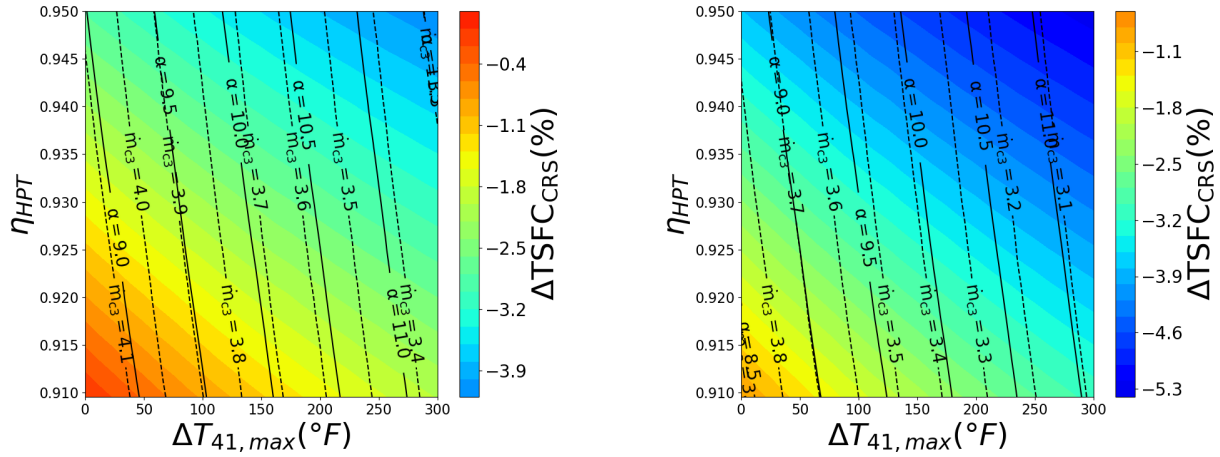

(a) OPR = 44.6 **(b) OPR = 50**

Fig. 5 KPP sensitivity to increased η_{HPT} and $T_{41,\mathbf{max}}$, $\Delta TCA = 0$

efficiency are accounted for in the results presented in Fig. 6c and Fig. 6d. As it was done in Fig. 5, trends are shown for the baseline and full success OPRs.

Figure 6a illustrates that increasing $T_{41,\max}$ at the base OPR and base $T_{\text{metal, HPT}}$ reduces fuel burn by up to about 1.4%, despite the significant increase in TCA required. Referring to the same figure, it is shown that fuel burn decreases with improved $T_{\text{metal, HPT}}$. When the effects of TCA on HPT efficiency are neglected, reducing TCA yields an overall efficiency benefit.

Referring back to Fig. 3, it becomes evident that the most significant cooling reduction and HPT efficiency improvement is achieved when $T_{\text{metal, HPT}}$ is raised to the full potential, while no adjustments are made to $T_{41,\max}$. The trends displayed in Fig.6c and Fig.6d reveal that when considering the influence of TCA on HPT efficiency, the most substantial reduction in fuel burn is achieved by elevating both temperatures. However, this approach ultimately encounters diminishing returns in fuel burn benefits, shedding light on the intricate interplay between HPT efficiency, TCA, and turbine inlet temperature, and the influence these parameters have on the cycle's thermal and overall efficiency. Notably, in cases where material temperature enhancements are relatively minor ($\Delta T_{\text{metal, HPT}} < 50°\text{F}$) raising the permissible inlet temperature could result in heightened fuel consumption. In such instances, the advantages of an elevated cycle temperature do not outweigh the associated increase in required TCA and the subsequent reduction in HPT efficiency.

In Fig. 6b and Fig. 6d it is again revealed that the benefits of increased cycle temperature are enhanced when accompanied by a heightened OPR, despite the increase in cooling flow temperature. In Fig. 6d it is shown that increasing OPR to 50 improves the maximum fuel burn reduction attainable by approximately 1% to approximately 3.8%. While this is a marked improvement, this fuel burn reduction, as measured at the propulsion system level, still falls below the minimum success criteria set by the HyTEC KPPs, 5%.

For all cases presented in Fig. 6, raising either of the temperatures considered results in a decreased core size and heightened BPR, noting that core size and BPR are much more sensitive to $T_{41,\max}$ when compared to $T_{\text{metal, HPT}}$. For the baseline OPR case, Fig.6c, in order to both minimize fuel burn and meet the HyTEC's minimum success criteria for core size, $T_{\text{metal, HPT}}$ must be increased by about 300°F and $T_{41,\text{ max}}$ must be increased by approximately 215°F. At this point, the reduction in the amount of TCA required results in a HPT efficiency improvement of about 1.6%. For the heightened OPR case, Fig.6d, to achieve the same fuel burn and core size goal, $T_{\text{metal, HPT}}$ must be increased by about 300°F and $T_{41,\text{ max}}$ must be increased by at least 90°F. At this point there is a significantly higher reduction in the amount of TCA required, resulting in a substantial HPT efficiency improvement–about 2.5%. In either OPR case, a BPR greater than 12 is not achievable.

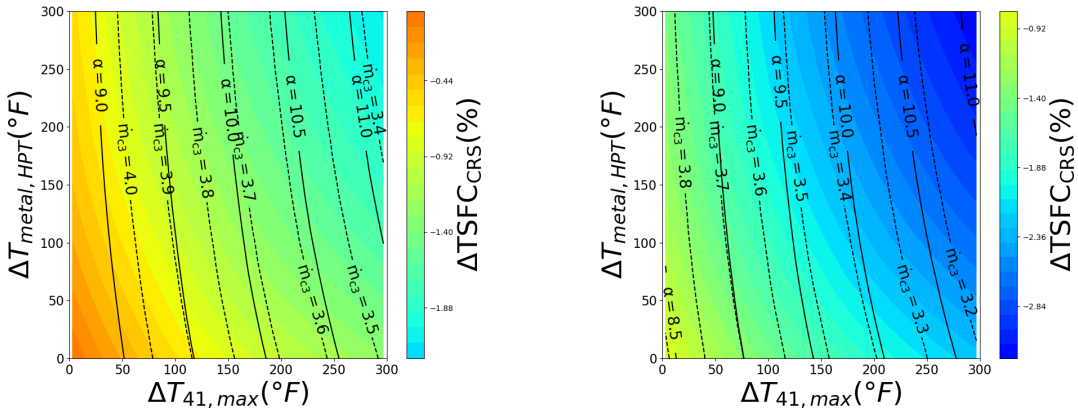

(a) OPR = 44.6, $\Delta\eta_{HPT} = 0$

(b) OPR = 50, $\Delta\eta_{HPT} = 0$

(c) OPR = 44.6, $\Delta\eta_{HPT} = f(\Delta TCA)$

(d) OPR = 50, $\Delta\eta_{HPT} = f(\Delta TCA)$

Fig. 6 KPP sensitivity to $T_{41,\text{max}}$ and $T_{\text{metal, HPT}}$, considering the influence of $T_{41,\text{max}}$ and $T_{\text{metal, HPT}}$ on TCA requirements, and the assumed effects of TCA on η_{HPT}

V. Vision engine

A. Engine cycle model

A notional vision engine is constructed as an exercise to quantify the isolated impact of small-core engine technologies on the HyTEC KPPs. Table 5 outlines the values used to modify the baseline engine model to produce the advanced cycle. A 10% increase is applied to the HPC pressure ratio (i.e. OPR). No polytropic efficiency penalty is applied to the HPC. Advancements made in HPT materials and cooling features are assumed to enable a 300°F improvement for $T_{\text{metal, HPT}}$ and a 215°F improvement for $T_{41,\text{max}}$. From these temperature changes, the amount of TCA required is reduced by 38% relative to the baseline amount. Based on the assumed effects of TCA on HPT efficiency, this reduction in cooling results in 1.53% HPT efficiency improvement. Advancements in HPT aerodynamics are assumed to improve the HPT efficiency by an additional 0.5%. Thus, in total, the HPT efficiency is increased by 2.03%. Figure 7 shows where the advanced cycle falls within a preliminary design space for the small-core engine, considering the improved $T_{metal,HPT}$ and the HPT efficiency gain from advanced aerodynamics.

Table 5 Vision Cycle Design Data

Technology	Parameter	Modification	Source
HPC - highly loaded stages	HPC Pressure Ratio	+10%	Input
HPC - advanced casing treatment	$\eta_{poly,HPC}$	-0%	Input
HPT - advanced materials	$T_{\text{metal, HPT}}$	+300°F	Input
HPT - advanced cooling	$T_{41,\text{ max}}$	+215°F	Input
	ΔTCA	−38%	Calculated
	η_{HPT}	+1.53%	Calculated
HPT - advanced aerodynamics	η_{HPT}	+0.50%	Input

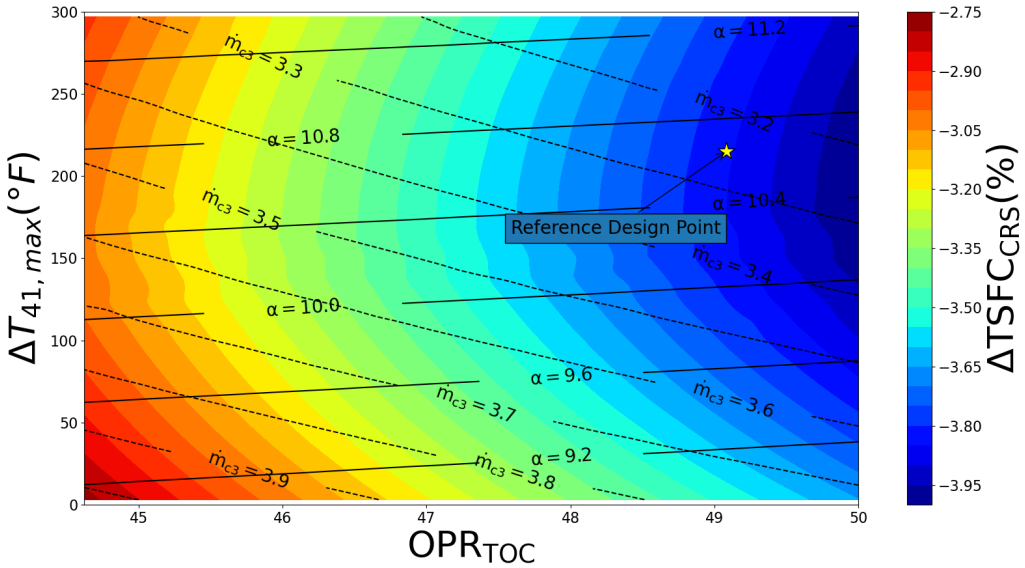

Fig. 7 Vision engine cycle design space with a reference design point highlighted at OPR = 49 and $\Delta T_{41,max}$ = 215°F

B. Engine weight and flowpath

The construction of the vision weight and flowpath model is derived from the reference WATE++ model. Despite a rise in OPR, the baseline turbomachinery stage counts are upheld in the vision design. This necessitates that the compressor and turbine stage loading be increased by 15% to 18%. In addition to improved stage loading, the vision WATE++ model incorporates CMCs as the material for the HPT vanes and combustor liner. Additional HPT mechanical design features are modified to represent blade aerodynamic improvements. With these modifications made, the estimated weight of the vision engine is approximately 440 lb less than the baseline. Table. 6 provides a comparison of some aeromechanical design features between the baseline model and the vision model. The WATE++ output diagrams for both engines are shown in Fig. 8.

Table 6 Comparison of Mechanical Design Parameters

Parameter	Baseline Model	Vision Model
Total engine pod weight (lbs)	8050	7610
Fan diameter (in.)	69.4	69.4
Nacelle maximum diameter (in.)	85.9	85.9
Engine length, fan face to nozzle (in.)	124	123
Fan/LPC/HPC/HPT/LPT stages	1-3-10-2-5	1-3-10-2-5
LP RPM	4800	4800
HP RPM	15000	16500
HPC last stage blade height (in.)	~ 0.50	0.45

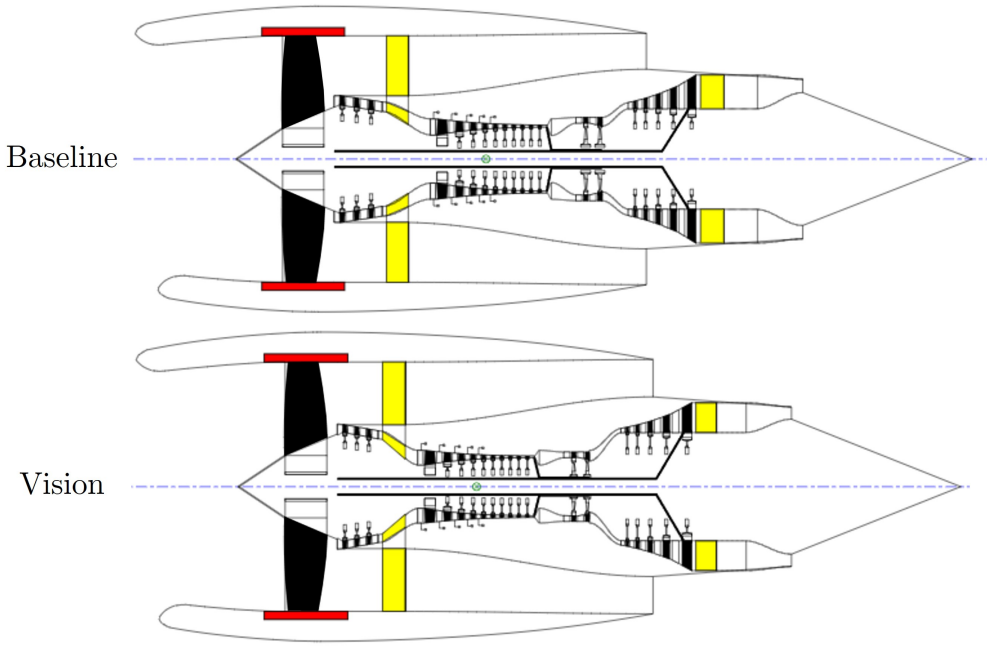

Fig. 8 WATE++ flowpath diagrams of the baseline and the vision engines

VI. Results

Figure 9 shows a breakdown of the influence that small-core engine technologies have on the KPPs, considering the notional vision cycle described in the previous section. The KPPs of the advanced engine are benchmarked against the baseline models. Due to the interconnected influence of HPT technologies on cycle performance, HPT technologies are integrated and assessed as a single group. KPP-1 (fuel burn) is first assessed as a change in TSFC at the cruise condition. Fuel burn is examined further by integrating the small-core engine and baseline aircraft and performing a vehicle mission analyses as described in Section III.D. The impact of reduced engine weight is also considered when evaluating fuel burn at the vehicle level. KPP-2 (BPR), KPP-3 (OPR), and KPP-6 (HPC exit corrected mass flow) are engine-level performance metrics. As such, the quantification of these metrics does not require any vehicle-level analyses. The assessment of BPR is conducted at the uninstalled sea level static condition, given that the baseline BPR is publicly quoted for this particular condition. HPC corrected mass flow is assessed at the cruise condition as core flow is generally lowest at this condition compared to the other high-power engine operating points. Comparative results for individual technologies are not provided for OPR as, for this analysis, changes to OPR are solely influenced by adjustments made to the HPC pressure ratio. The baseline HPC pressure ratio is raised by 10% for the advanced cycle,

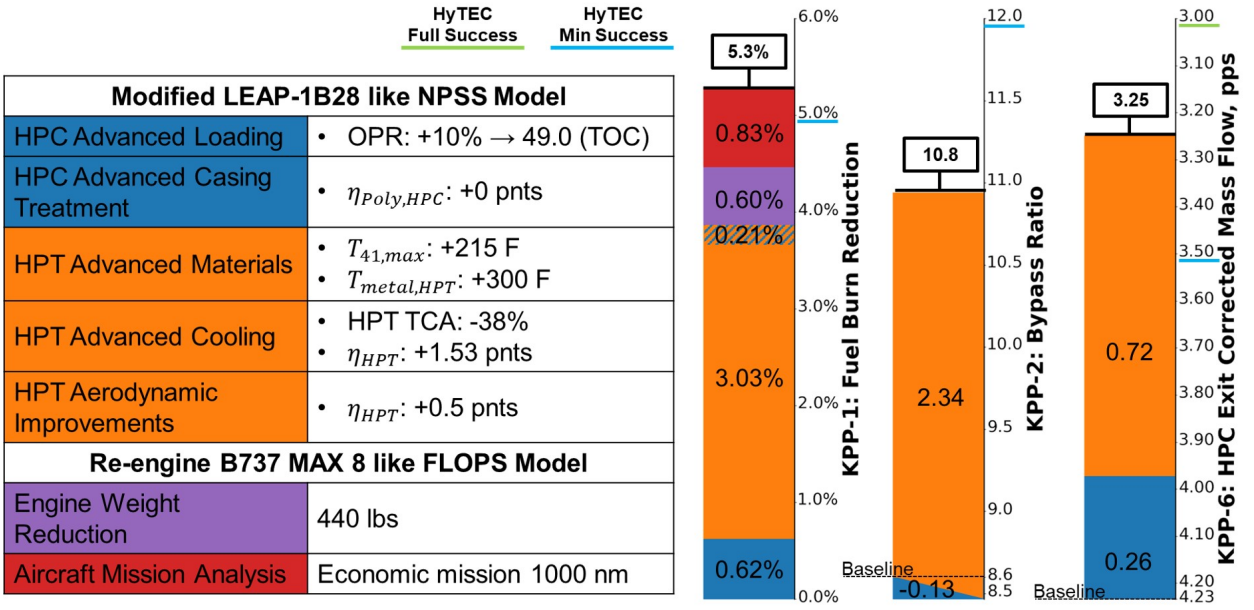

Fig. 9 Impact of small-core technologies on key performance parameters of the LEAP and B737 MAX 8 like models, assessed using notional engine design changes

resulting in an OPR of 49.0 at the TOC condition.

The results presented in Fig. 9 show that, overall, a 5.3% fuel burn reduction is enabled by the integration of small-core engine technologies. The percentage of fuel burn reduction that is attributed to each technology is found by a 'first on' approach where an individual technology is added to the baseline and the improvement is calculated. When only HPC technologies are integrated, a 0.62% reduction in TSFC at cruise is the result. When only HPT technologies are integrated, TSFC is reduced by 3.03%. Integrating both HPC and HPT technologies simultaneously yields a 3.86% TSFC reduction. Thus, an additional 0.21% TSFC reduction is enabled by both HPC and HPT technologies. When the baseline aircraft is modeled considering the thermodynamic performance of the advanced engine, the total mission block fuel burn is reduced by 4.7%, a 0.83% improvement over the 3.86% reduction in TSFC. Finally, when the baseline aircraft is modeled with both the updated engine performance and the reduced engine weight, the total mission block fuel burn is reduced by 5.3%. Thus, as additional 0.6% reduction in fuel burn is attributed to the reduced engine weight. Overall, the total fuel burn reduction assessed using the advanced engine, 5.3%, exceeds the minimum HyTEC success criteria of 5%.

Considering BPR, when only HPC technologies are integrated, BPR is reduced by about 0.01 points. When only HPT technologies are considered, the BPR increases by 2.34 points up to a BPR of 10.94 from the baseline BPR of 8.6. Consequently, when HPC technologies are integrated along with HPT technologies, the BPR only increases by a total of 2.21 points, a 0.13 point reduction from what was achievable with only HPT technologies, making the BPR of the advanced engine 10.8. This BPR falls short of the HyTEC minimum success criteria of BPR > 12.

For HPC exit corrected core flow, when only considering the integration of HPC technologies, the corrected flow is reduced by 0.26 lbm/s. When only HPT technologies are integrated, the corrected flow is reduced by about 0.72 lbm/s. When both HPC and HPT technologies are integrated simultaneously, the corrected flow is reduced by a total of 0.98 lbm/s. Thus, HPC exit corrected flow is reduced from the baseline value of 4.23 lbm/s down to 3.25 lbm/s for the advanced engine. Having a corrected core flow of 3.25 lbm/s exceeds the HyTEC minimum success criteria for core flow, which is 3.5 lbm/s.

VII. Summary

This study has demonstrated an approach to examining the quantifiable impact of small-core technologies on turbofan performance and aircraft fuel burn. The evaluation process involved a model-based systems analysis approach, in which small-core advancements were integrated into reference turbofan and aircraft systems models, forming a conceptual vision system. Performance assessments were conducted at both the engine and aircraft levels, considering key performance metrics, including engine bypass ratio, overall pressure ratio, high-pressure compressor exit corrected mass flow, and aircraft fuel burn. The approach considered HPC technologies that would allow the baseline OPR to increase from 44.6 to 50 without encountering an HPC polytropic efficiency penalty. Also considered were HPT technologies that improve the allowable turbine inlet temperature, reduce HPT cooling air requirements, and improve HPT efficiency. Additionally, the approach considered aeromechanical design changes which reduce the size and weight of the core, and overall engine by extension. It was demonstrated that a combination of both compressor and turbine technologies is required to meet the minimum success criteria defined by the HyTEC project. It is important to emphasize that the results presented here are provisional and should not be construed as the definitive outcomes of the HyTEC project. These results rely on specific assumptions related to the development and integration of core technologies explored within the initial phases of the HyTEC project. As such, the information contained herein comprises initial estimates for a selection of the HyTEC project's anticipated outcomes. These figures are subject to revision once technology development has been concluded. Future research could expand the scope of this study by investigating a broader spectrum of advanced technologies and their integration with novel engine and aircraft designs.

Acknowledgments

The authors extend their gratitude to NASA's AATT and HyTEC projects for funding and supporting this study. The team also wishes to express their sincere appreciation for the invaluable technical guidance provided by Scott Jones, Eric Hendricks, and Mike Tong from NASA Glenn Research Center, whose mentorship and insights significantly contributed to the success of this research endeavor.

References

[1] "United States 2021 Aviation Climate Action Plan," Federal Aviation Administration, November 2021. URL https://www.faa.gov/sustainability/aviation-climate-action-plan, [cited 2 November 2023].

[2] NASA, "NASA Hybrid Thermally Efficient Core (HyTEC) Project, NASA Glenn Research Center (GRC) NASA Research Announcement (NRA) for Phase 1 Technology Development," https://sam.gov/opp/e9944bbafcff43d0a0a860158dbb3d9b/view, 2021. ANNOUNCEMENT NUMBER: 80GRC021N0001.

[3] "NASA, US Industry Accelerate Advancement of Small Core Aircraft Engines," NASA, 2021. URL https://www.nasa.gov/feature/glenn/2021/nasa-us-industry-accelerate-advancement-of-small-core-aircraft-engines, [cited 2 November 2023].

[4] Claus, R. W., Evans, A. L., Lytle, J. K., and Nicholas, L. D., "Numerical Propulsion System Simulations," *Computing Systems in Engineering*, 1991, pp. 357–364. https://doi.org/10.1016/0956-0521(91)90003-N.

[5] Tong, M. T., and Naylor, B. A., "An Object-Oriented Computer Code for Aircraft Engine Weight Estimation," ASME Turbo Expo: Power for Land, Sea, and Air, Berlin, Germany, 2008. https://doi.org/10.1115/GT2008-50062.

[6] McCullers, L. A., "Aircraft Configuration Optimization Including Optimized Flight Profiles," NASA CP-2327, April 1984, pp. 395–412.

[7] "Type Certificate Data Sheet E00088EN," Federal Aviation Administration, November 2019. URL https://drs.faa.gov/browse/, [cited 2 November 2023].

[8] "ICAO Aircraft Engine Emissions Databank," European Union Aviation Safety Agency, June 2023. URL https://www.easa.europa.eu/en/domains/environment/icao-aircraft-engine-emissions-databank, [cited 2 November 2023].

[9] "737 MAX Airplane Characteristics for Airport Planning," Boeing, March 2023. URL https://www.boeing.com/commercial/airports/plan_manuals.page, [cited 2 November 2023].

[10] Thacker, R., and Blaesser, N. J., "Modeling of a Modern Aircraft Through Calibration Techniques," *AIAA Paper 2019–2984*, June 2019. https://doi.org/10.2514/6.2019-2984.

[11] Hahn, A., "Vehicle Sketch Pad: A Parametric Geometry Modeler for Conceptual Aircraft Design," 48th AIAA Aerospace Sciences Meeting Including the New Horizons Forum and Aerospace Exposition, AIAA, Orlando, Florida, 2010. https://doi.org/10.2514/6.2010-657.

[12] Schutte, J. S., "Simultaneous Multi-Design Point Approach To Gas Turbine On-Design Cycle Analysis For Aircraft Engines," Ph.D. thesis, The Georgia Institute of Technology, Atlanta, GA, May 2009.

[13] Daggett, D. L., Brown, S. T., and Kawai, R. T., "Ultra-Efficient Engine Diameter Study," NASA/CR—2003-212309, May 2003.

[14] Gauntner, J. W., "Algorithm for Calculating Turbine Cooling Flow and the Resulting Decrease in Turbine Efficiency," NASA TM—81453, February 1980.

[15] Suder, K. L., Delaat, J., Hughes, C., Arend, D., and Celestina, M., "NASA Environmentally Responsible Aviation Project's Propulsion Technology Phase I Overview and Highlights of Accomplishments," 51st AIAA Aerospace Sciences Meeting including the New Horizons Forum and Aerospace Exposition, Grapevine, Texas, 2013. https://doi.org/10.2514/6.2013-539.

[16] Jones, S. M., Haller, W. J., and Tong, M. T., "An N+3 Technology Level Reference Propulsion System," NASA TM—2017-219501, May 2017.

[17] DiOrio, A. G., "Small Core Axial Compressors for High Efficiency Jet Aircraft," Master's thesis, Massachusetts Institute of Technology, Cambridge, MA, September 2012.

[18] Michael, C. H., Martha, H. J., James, D. K., and Dongming, Z., "Evaluation of Ceramic Matrix Composite Technology for Aircraft Turbine Engine Applications," 51st AIAA Aerospace Sciences Meeting including the New Horizons Forum and Aerospace Exposition, Grapevine, Texas, 2013. https://doi.org/10.2514/6.2013-539.

[19] Walsh, P. P., and Fletcher, P., *Gas Turbine Performance*, 2nd ed., Blackwell Science Ltd, Oxford, UK, 2004.

[20] Kerrebrock, J. L., *Aircraft Engines and Gas Turbines*, 2nd ed., MIT Press, Cambridge, MA, 1992.